PARTIAL SURVEY OF CODES FOR HIGH FREQUENCY SCATTERING FROM FACET MODELS OF RADAR TARGETS

Michael A. Richards
Nichols Research Corporation
Shalimar, Florida 32579

ABSTRACT

In this work, four high-frequency electromagnetic scattering codes are surveyed with regard to their capabilities and limitations for the calculation of the radar cross section (RCS) of facet models of targets. The codes discussed are MISCAT, NRCPTD, McPTD, and Xpatch. All of these codes utilize the physical theory of diffraction (PTD) to approximate the field scattered from the target. A short discussion of the modeling features of each code is given and some sample numerical results are generated. It is concluded that, of the models considered here, Xpatch possesses the most comprehensive modeling features available, with no loss in accuracy over the other codes.

1.0 INTRODUCTION

Choosing a high-frequency electromagnetic scattering code to accurately describe the radar signature of a given target can be a substantial endeavor. Often, the modeller will utilize the "familiar" code even when it is not the tool best suited to the objective. Also, when there is a lack of accessible information on available codes, additional effort may be expended in modifying existing models or in developing new codes to perform a specific task. However, as users become more familiar with the available models, the need to modify existing codes and develop new models is sometimes decreased.

The purpose of this paper is to familiarize the reader with the aforementioned scattering codes. It is acknowledged that this survey is not comprehensive in that only four PTD-based computer models are considered. Other excellent models are available that utilize the PTD and/or the Geometrical Theory of Diffraction (GTD).

2.0 TARGET MODELING AND SCATTERING CODES

In this report, four active far-field electromagnetic scattering codes are discussed. These are MISCAT, McPTD, NRCPTD, and Xpatch. All of these codes are written in FORTRAN and employ the PTD to determine the scattering signature of radar targets. The PTD does not include higher order edge diffractions or creeping wave effects. These codes do not model the scattering from extended targets. The incident radiation is assumed to be a uniform plane wave with constant magnitude and polarization over the target surface, and the scattered radiation is assumed to be a spherical wave emanating from a single location. Also, these models do not currently possess the capability to comprehensively analyze rough surfaces in that no incoherent scattering pheonomena are modeled. However, the Xpatch code does have the capability to associate a user-defined reflection coefficient with the scattering surface as discussed in section 2.4. Some of the assumptions, limitations, and modeling features of these codes are discussed in the following sections.

2.1 <u>MISCAT</u>

The MISCAT scattering code was written by Northrop Corporation for the U.S. Army

Missile and Space Intelligence Center (MISC) [1]. The code was written for the purpose of calculating the RCS of complex airborne targets such as aircraft and missiles.

The current version of the code [2] calculates the RCS of conducting or coated conducting targets. The RCS calculation can be monostatic or bistatic, and both co-polarized and cross-polarized scattering signatures can be determined. The target geometry is modeled as a set of primitives (plates, polygonal cylinders, elliptical cylinders, and bodies specified by surface contours) and the total body RCS is obtained by coherently summing the contribution due to each geometrical primitive.

The code can be used to predict the scattering signature of convex targets. Its major limitations are in the shadowing calculation and single-bounce scattering assumption. The shadowing of a facet is calculated using only the facet normal vector. That is, the shadowing of one portion of the body by another portion is not analyzed. Another limitation of the code comes about due to the method employed to describe the target geometry. The format employed is quite general but also quite bulky and no automatic edge/wedge extraction feature is provided. (If the target under consideration can be modeled using some of the higher-order geometrical primitives, then an automatic wedge contribution calculation can be performed.) The code is quite useful for the purpose for which it was intended -- analysis of airborne targets. However, analysis of these target at aspects associated with body inlets, cavities, and other interacting surfaces can not be performed reliably.

2.2 NRCPTD

This acronym (NRCPTD) is used to signify the author's efforts at RCS prediction of complex targets [3]. At present, NRCPTD is not a single code but consists of separate modules for analyzing different contributions of the scattering process. Some of the features of these codes will now be discussed.

The physical optics (PO) currents depends upon an approximation of the geometrical optics (GO) field on the surface of the illuminated region of the target. When the body can be approximated by a perfect electric conductor (PEC), the GO field is just twice the tangential incident magnetic field since the total tangential electric field is zero on the surface of the body. To allow for the modeling of nonperfectly conducting bodies as well as RAM coated targets, we have utilized the exterior equivalent Fresnel reflection coefficients to obtain the GO surface field.

The material composition of the target can be quite general but not completely arbitrary. The target can consist of PEC components and/or conducting components coated with arbitrary dielectric layers and/or lossy dielectric components coated with dielectric layers. Transparent body components can not be treated with this code.

There exists a shadow boundary on the target which divides the illuminated region from the shadowed region. For a simple convex body, we can distinguish between the illuminated and shadowed regions by use of the body's normal vector. If the target is complex, more elaborate steps can be taken to identify the illuminated portion of the body. The method implemented in this model is approximate but still quite useful. It consists of treating each facet of the target as hidden or illuminated dependent upon whether the centroid of the facet is hidden or illuminated. Clearly, this is an approximation but one that can be used to obtain any desired level of accuracy by adjusting the facet size. We have also retained the simpler, and computationally faster, surface normal approximation to the shadowed region as a user option.

In using the PTD to approximate the high-frequency scattering signature of a target, it is necessary to know the location and orientation of the geometrical discontinuities (wedges and edges) on the body. In this code an algorithm was implemented to extract exterior wedges and edges (wedges with zero interior angle) from a facet file. The extraction routine locates connected facets and then checks the angle between the adjoining facet normals to decide if a "true" wedge or edge is formed. The angle between the normals for which a wedge is determined is a user-defined parameter and can be set based on how finely the target is discretized.

Since the wedge extraction algorithm looks for wedges and edges when the vertices of two connected facets are the same, it is possible to construct a wedge geometry that the algorithm will not process correctly. For instance, when a wedge is formed by two facets whose vertices are offset such that the wedge does not run the full length of both facets, the wedge will not be found.

In summary, this code employs the PTD to predict the scattered field and associated RCS of complex targets. The target is modeled by a set of triangular facets. The total body contribution is obtained by summing the contribution due to each facet. The facets can be conducting or can be coated with material layers. Geometrical optics is used to approximate the surface field on the target. From the GO surface field, the equivalent currents are calculated. Integrating over the equivalent currents provides the PO approximation to the scattered field. Edge effects can be included for conducting body components. The RCS determined by the code can be monostatic or bistatic and both co-polarized and cross-polarized scattering signatures can be calculated. Angle scans and frequency sweeps can be easily performed.

2.3 McPTD

McPTD consists of a family of component computer codes for the high-frequency computation of the scattered field/RCS of complex targets [4]. The codes were written primarily by S. W. Lee at the University of Illinois and have undergone several upgrades since they were first distributed in 1990. They are currently being distributed by Dr. Lee's company, DEMACO, and by the electromagnetic code consortium (EMCC).

The codes analyze the scattering from a variety of geometrical components ranging from flat facets to numerically-defined, CAD-generated surfaces. A main routine exists for the summation of the field scattered from the different target components.

The primary limitations of the code lie in its inability to model multiple-bounce scattering mechanisms and in its shadowing capability. While the ability to perform accurate shadowing is available, the code uses an inefficient process, just as in NRCPTD. Nevertheless, McPTD is a more sophisticated modeling tool than both MISCAT and NRCPTD discussed previously.

Since the McPTD family of codes is written by the same author as the Xpatch codes to be discussed next, no numerical results generated via McPTD will be given here. Also, McPTD is essentially a subset of the more sophisticated modeling tool, Xpatch.

2.4 Xpatch

Xpatch consists of a set of codes written primarily by S. W. Lee [5]. The codes analyze the scattering signatures of complex targets in both the frequency and time domains. Shown in Table 1 is a list of some of the capabilities of the various Xpatch modules.

Notice that Xpatchl and Xpatch2 are frequency-domain codes while Xpatch3 and Xpatch4 are time-domain codes. Although conversion from one domain to another can be accomplished via the Fourier transform, each domain offers computational advantages. For instance, modules 3 and 4 are time-domain codes and do not easily model material parameters.

The Xpatch codes provide for a range of target modeling geometrical primitives. Modules 1 and 3 employ a triangular facet description of the target geometry in ACAD format [6]. (These ACAD facet files can be easily converted to formats applicable for input to MISCAT and NRCPTD). Modules 2 and 4 employ a numerical description of the target surface. The initial graphics exchange specification (IGES) can be used to describe target geometries to the code. Also, the code can utilize constructive solid geometry (CSG) models created with BRL-CAD [7].

The frequency-domain codes (modules 1 and 2) can model the edge diffraction contribution for conducting edges. This contribution is for a single-bounce interaction. That is, only the field originally incident on the target can produce an edge diffraction contribution. Parameter extraction for wedges and edges can be performed by a component preprocessing code.

All modules of the Xpatch family can utilize a shooting and bouncing ray (SBR) algorithm [8,9]. In this approach a dense grid of rays is shot at the target. The rays are traced throughout the target using GO and then a PO integration over the equivalent currents on the last interacting surface is performed. Perfect specularity is assumed in the ray tracing. Shadowing is automatically performed in the SBR analysis.

When using facet models generated via CAD packages, errors in the direction of the facet normal vectors is a common occurrence. Using the Xpatch codes in SBR mode eliminates the need to know the direction of the facet normal vector.

Another feature of the Xpatch code is its capability to read a set of angular and frequency dependent reflection coefficients and associate these coefficients with various facets on the target. These coefficients are then used in the ray tracing and equivalent current computation. It appears feasible to use this feature of the code to model the reduction in the coherent component of the RCS of a slightly rough target. This has application in the millimeter wave (MMW) region of the spectrum.

The documentation provided with the Xpatch codes is currently limited. No comprehensive technical description of the techniques and approximations employed is given. However, some documentation is given within the input file structure as well as in an example problem set provided with the codes. For researchers already familiar with the modeling of high-frequency electromagnetic scattering, enough documentation is provided to enable the user to become proficient with the code.

The Xpatch codes are currently being utilized on Silicon Graphics machines. The main routines are written in FORTRAN and can be ported to other machines with minimal effort. If a PC is to be used, then a compiler is needed that can access extended memory. Some utility codes (format conversion, wedge parameter extraction, etc.) are written in C and no source code is provided.

The Xpatch codes have other features which have not been fully discussed here. For some comparisons of measured results to numerical Xpatch simulations, the reader can consult some recent literature [10].

2.5 Numerical Results

In this section some numerical results will be considered. These examples serve as a partial validation of the newer codes against the more established models and also illustrate some of the features and limitations of the codes. The frequency of the incident radiation in the following examples is taken to be 1.0 GHz in all cases and is chosen for illustration purposes. While the PTD would provide a more accurate estimate of the true RCS of the targets considered below if the frequency were increased an order of magnitude, the resulting plots would be unnecessarily dense. Hence, the lower frequency was preferred for these comparisons.

Numerical comparisons other than the ones shown below have been made. While some of these comparisons have utilized more complex and realistic geometric models, the resulting predictions are readily extrapolated from the examples given below. Please note that in making comparisons with the Xpatch codes, only results generated via Xpatch1 will be shown here. The other Xpatch modules have many interesting features and capabilities as outlined above but tend to be beyond the scope of this comparison.

2.5.1 PEC Plate

Consider the thin square plate shown in Fig. 1. It is 1.0 m on a side and is taken to be perfectly conducting. The co-polarized monostatic RCS of the plate has been calculated using the scattering codes and the results are shown in Fig. 2. The incident field is a vertically polarized plane wave. The zenith angle is $\theta = 90^\circ$ (x-y plane) and the azimuth angle is varied from 0° (broadside) to 90° (grazing).

The calculations were performed using the PTD and for reference purposes the method of PO (no edge contribution). Notice that at broadside, the RCS has a value of 21.4 dBsm and agrees with the analytical PO result of $4\pi(A_p/\lambda)^2$, where A_p is the area of the plate and λ is the wavelength of the incident radiation. Furthermore, notice that the first sidelobe is 13.2 dB down from the maximum as is typical for rectangularly-shaped scatterers and uniformly illuminated apertures. The PO result is a fairly accurate estimate for the first few sidelobes except in the prediction of the nulls. After the first few lobes, the edge starts to dominate the response and the PO approximation yields an inaccurate result. Finally, notice that for this simple target, all three PTD scattering codes agree well for all aspects considered.

2.5.2 RAM Coated Plate

In this example a coated body will be analyzed. Consider the rectangular plate shown in Fig 3. The plate is of width 2.0 m and height 3.0 m and is coated with a broadband RAM. The coating is 1.0 cm thick with relative permittivity and permeability of $\varepsilon_r = \mu_r = 2 - j\,5$. This RAM does not exist in practice but is used for the purpose of illustration.

The PO approximation to the co-polarized (VV) monostatic RCS of the coated plate has been computed and the results are shown in Fig. 4. The zenith angle is held constant at $\theta = 90^\circ$ (x-y plane) and the azimuth angle is scanned from 0° to 90°. Shown for comparison is the PO approximation to the RCS of a PEC plate of the same size. Notice that the RAM coating significantly reduces the RCS from that of the uncoated plate. At normal incidence, the amount of reduction is seen to be 18.2 dB corresponding to the reduced Fresnel reflection coefficient. As in the previous example, the first sidelobe is 13.2 dB down from the maximum and the first null occurs at an azimuth angle of $\phi = \sin^{-1}(\lambda/2w)$ where w is the width of the plate. Observe that all scattering models again produce equivalent results in this case.

2.5.3 Dihedral Corner

Consider the dihedral corner reflector shown in Fig. 5. It is of length 2.0 m in each of the x, y, and z dimensions. The co-polarized (VV) monostatic RCS of the corner has been calculated and the results are shown in Fig. 6. The zenith angle is held constant at $\theta_o = 90^\circ$ (x-y plane) and the azimuth angle is varied from 0° (normal to face 2) to 90° (normal to face 1). Only scattering from the interior of the corner has been considered and all edge diffraction effects have been ignored. Although edge diffraction effects can be important for scattering from the exterior corner (wedge), the single and double-bounce scattering mechanisms dominate the response of the interior corner.

Shown in Fig. 6 are the results of three different solution procedures. First, the analytical solution to the RCS is shown. This represents the combined single-bounce PO approximation and the double-bounce GO/PO approximation. Also shown in this figure is the single-bounce approximation available with any of the codes. Finally, the Xpatch code was used in SBR mode (SBR/2 BOUNCE) to approximate the RCS of the corner. In the SBR mode, 10 rays/wavelength were shot at the target and 2 bounces were allowed. Notice the results of the SBR analysis agree very well with the analytical result. Furthermore, notice that the single-bounce PO approximation is inadequate for describing the response of the interior corner over most of the aspects shown.

The Xpatch code is the only model considered that can provide an adequate description of the response of the dihedral corner. The other scattering codes considered (MISCAT, McPTD, and NRCPTD) do not attempt to analyze multiple bounce scattering. While the effect of multiple bounces is not always an important contributory mechanism, the errors introduced by neglecting them can, for some targets, be significant.

The SBR mode of the Xpatch code requires that a dense grid of rays be shot at the target. The density of the ray grid governs the accuracy of the approximation with a dense grid providing more accurate results than a coarse grid. In the previous example, the density of the grid was 100 rays per square wavelength. Shown in Fig. 7 is the RCS of the corner calculated via Xpatch in SBR mode using a grid density of 2 rays/wavelength (4 rays per square wavelength). Also shown for comparison purposes is the analytical calculation of the RCS. Notice that the Xpatch solution is degraded somewhat from the previous example but still provides what for some cases could be an adequate approximation.

2.6 Model Survey Summary

A summary of the capabilities and limitations of the various codes discussed in this report is given in Table 2. Of the codes considered, MISCAT is currently the most trusted (for a limited set of targets) and best documented while Xpatch provides the most comprehensive modeling features. Xpatch has the capability to model multiple bounce scattering as well as shadowing. While NRCPTD and McPTD can perform global shadowing checks, they are not as efficient in this regard as the Xpatch codes.

ACKNOWLEDGEMENT

The author would like to thank Major Keith Trott (USAF) of WL/MNGS at Eglin AFB for his encouragement to write this paper and for his proofreading of an earlier version of the work. Also, the author owes John Watson of Nichols Research Corporation much thanks for providing direction to undertake this work. This work was supported through the Data Analysis and Modeling (DAAM) Program (F08635-91-C-0110) with the Armament Directorate of Wright Laboratory located at Eglin, AFB.

REFERENCES

1. T. J. Kim and H. B. Tran, Monostatic and Bistatic Radar Cross Section Analysis, Vol. 1 - The High Frequency Electromagnetic Scattering Theory, Technical Report NOR-82-215, Dec. 1982.

2. S. C. Gibson and T. J. Kim, Radar Cross Section Analysis by the Physical Theory of Diffraction, Vol. 2 - User's Manual, Technical Report NOR-89-56, Mar. 1989.

3. M. Richards, IRMA Active MMW Channel Upgrade Investigations, Technical Report NRC-TR-93-042, May 1993.

4. S. W. Lee, McPTD-2.1: A High Frequency RCS Computation Code Based on Physical Theory of Diffraction, Technical Report, DEMACO, Mar. 1992.

5. S. W. Lee, Xpatch: A High Frequency RCS Computation Code for Facet Targets and Curved Patches, Technical Report, DEMACO, Aug. 1992.

6. Advanced Computer Aided Design User's Manual-7.2, General Dynamics, Fort Worth, TX, Jan. 1991.

7. The Ballistics Research Laboratory CAD Package-3.0, Aberdeen Proving Ground, MD, 1988.

8. H. Ling, R. Chou, and S. W. Lee, "Shooting and Bouncing Rays: Calculating the RCS of an Arbitrarily Shaped Cavity," IEEE Trans. Antennas Propagat. pp. 194-205, Feb. 1989.

9. J. Bauldauf, S. W. Lee, L. Lin, S. K. Jeng, S. M. Scarborough, and C. L. Yu, "High Frequency Scattering from Trihedral Corner Reflectors and Other Benchmark Targets: SBR Versus Experiment," IEEE Trans. Antennas Propagat. pp. 1345-1351, Sept. 1991.

10. E. M. Miller, "Validation of Xpatch Radar Signature Prediction Using Flat Flat Facet Geometries," MS Thesis, Air Force Institute of Technology, Dec. 1992.

Table 1. Capabilities of Xpatch family of scattering codes.

Code / Feature	Xpatch1	Xpatch2	Xpatch3	Xpatch4
Domain	Frequency	Frequency	Time	Time
Modeling Primitives	Facet	CSG/IGES	Facet	CSG/IGES
Coatings	Yes	Yes	No	No
Edge Diffraction	Yes	Yes	No	No
Shadowing	Yes	Yes	Yes	Yes
Multiple Bounces	Yes	Yes	Yes	Yes
Uses	RCS and Range Profile	RCS and Range Profile	Range profile and SAR*	Range profile & SAR*

* Not conventional SAR but images are similar.

Table 2. Capabilities of EM scattering codes surveyed.

Feature / Code	**Surface Coatings**	**Wedge Extraction**	**Wedge Effects (PEC)**	**Global Shadowing**	**Multiple Bounces**
MISCAT	**Yes**	**No**	**Yes**	**No**	**No**
NRCPTD	**Yes**	**Yes**	**Yes**	**Yes ***	**No**
McPTD	**Yes**	**Yes**	**Yes**	**Yes ***	**No**
Xpatch	**Yes**	**Yes**	**Yes**	**Yes**	**Yes**

* Not handled as well as in Xpatch

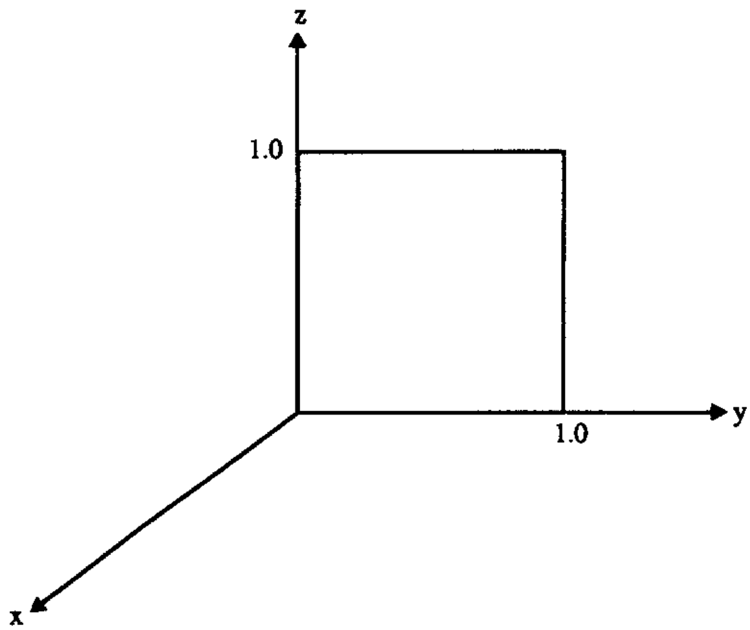

Fig. 1. Thin conducting square plate.

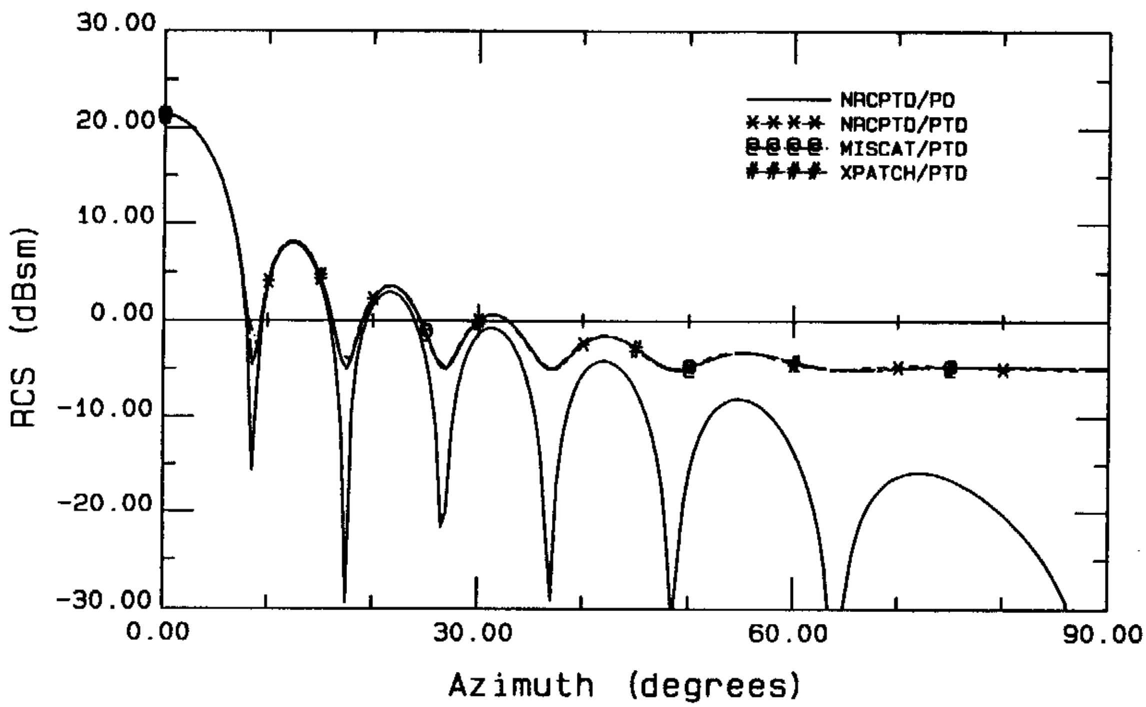

Fig. 2. Co-polarized (VV) monostatic RCS of a square (1m x 1m) conducting plate. The zenith angle is held constant at $\theta = 90^\circ$ and the azimuth angle is varied from 0° to 90°.

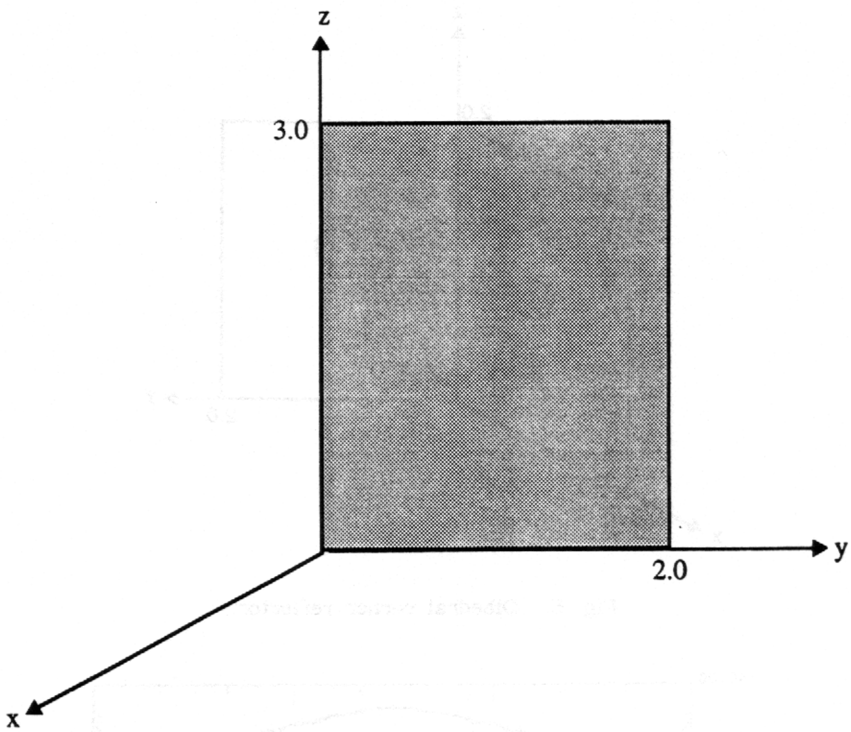

Fig. 3. Rectangular plate of height 3.0 m and width 2.0 m coated with a broadband RAM. The coating is 1.0 cm thick with dielectric properties $\hat{\varepsilon}_r = \hat{\mu}_r = 2 - j\,5$.

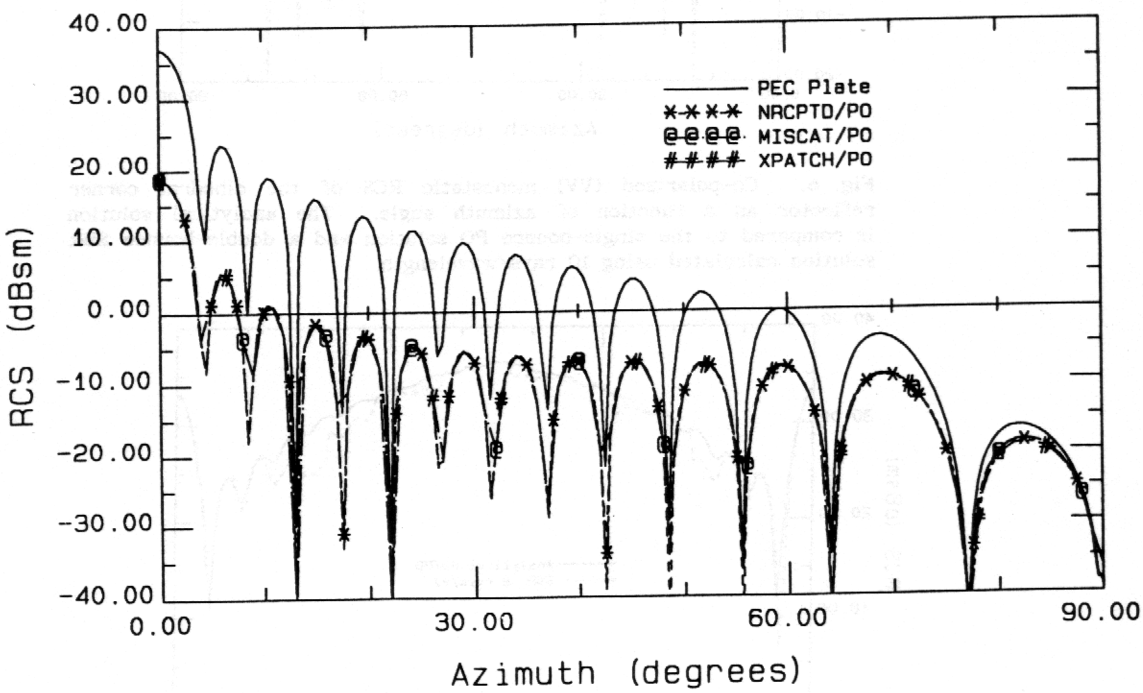

Fig. 4. PO approximation to the RCS of the RAM coated plate. Shown for comparison is the PO approximation to the RCS of a PEC plate of the same size.

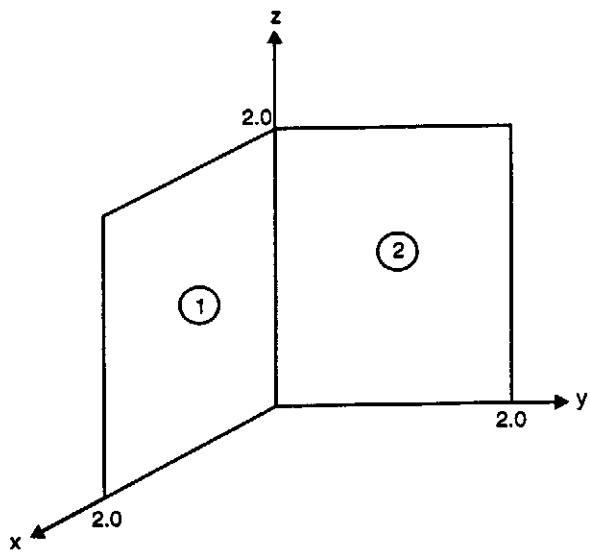

Fig. 5. Dihedral corner reflector.

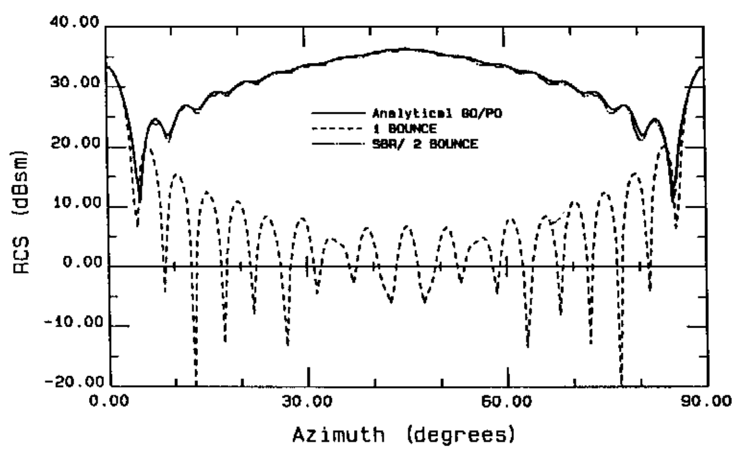

Fig. 6. Co-polarized (VV) monostatic RCS of the dihedral corner reflector as a function of azimuth angle. The analytical solution is compared to the single-bounce PO solution and a double-bounce SBR solution calculated using 10 rays/wavelength.

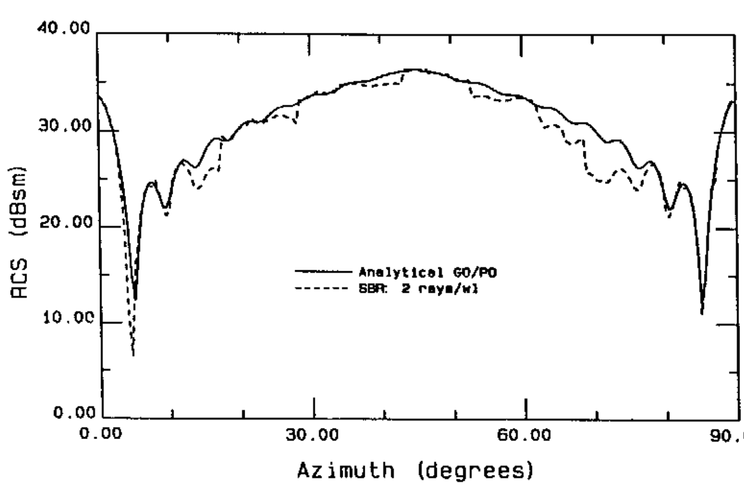

Fig. 7. Co-polarized (VV) monostatic RCS of the dihedral corner reflector obtained from an analytical solution and the SBR technique with 2 rays/wavelength.